Primljen / Received: 15.1.2021.
Ispravljen / Corrected: 29.3.2021.
Prihvaćen / Accepted: 22.4.2021.
Dostupno online / Available online: 10.6.2021.

Experimental investigation of preload losses in high strength bolts under cyclic loading

Authors:

Assist.Prof. **Nenad Fric**, PhD. CE
University of Belgrade, Serbia
Faculty of Civil Engineering
fric@imk.grf.bg.ac.rs
Corresponding author

Prof. **Milan Veljković**, PhD. CE
Delft University of Technology, Netherlands
Department of Engineering Structures
m.veljkovic@tudelft.nl

Assoc.Prof. **Zoran Mišković**, PhD. CE
University of Belgrade, Serbia
Faculty of Civil Engineering
mzoran@imk.grf.bg.ac.rs

Prof.emer. **Dragan Buđevac**, PhD. CE
University of Belgrade, Serbia
Faculty of Civil Engineering
budjevac@grf.bg.ac.rs

Original scientific paper

Nenad Fric, Milan Veljković, Zoran Mišković, Dragan Buđevac

Experimental investigation of preload losses in high strength bolts under cyclic loading

Slip-resistant shear connections with preloaded bolts have traditionally been used in steel structures exposed to cyclic. Hence, shear load is transferred through friction surfaces rather than through contact between the bolt surface and the hole. The main influencing parameters determining slip resistance of the connection are the friction between contact surfaces and the bolt preload level. This paper presents an experimental study of preloaded bolted connections under cyclic load, the main objective being to investigate the influence of cyclic load on the losses of preload force in high strength bolts and lock bolts.

Key words:
high strength bolt, preload force, preload loss, slip factor, cyclic load

Izvorni znanstveni rad

Nenad Fric, Milan Veljković, Zoran Mišković, Dragan Buđevac

Eksperimentalno istraživanje gubitaka prednapinjanja u visokovrijednim vijcima pod cikličkim opterećenjem

Posmični spojevi otporni na proklizavanje s prednapetim vijcima tradicionalno se koriste u čeličnim konstrukcijama izloženim cikličkom opterećenju. Stoga se posmično opterećenje prenosi preko tarnih površina, a ne kroz kontakt između površine vijka i rupe. Glavni utjecajni parametri koji određuju otpornost na proklizavanje spoja su trenje između kontaktnih površina i razina prednapinjanja u vijcima. U radu su predstavljeni rezultati eksperimentalnih ispitivanja prednapetih vijčanih spojeva pod cikličkim opterećenjem s glavnim ciljem ispitivanja utjecaja cikličkog opterećenja na gubitke sile prednapinjanja u visokovrijednim vijcima i vijcima s uređajima za sprječavanje odvrtanja.

Ključne riječi:
visokovrijedni vijak, sila prednapinjanja, gubitak prednapinjanja, faktor proklizavanja, cikličko opterećenje

Wissenschaftlicher Originalbeitrag

Nenad Fric, Milan Veljković, Zoran Mišković, Dragan Buđevac

Experimentale Forschung von Verlusten bei der Vorspannung in den hochwertigen Schrauben, welche unter der zyklischen Belastung stehen

Schiebeverbindungen, welche widerstandsfähig gegen das Durchrutschen sind und die vorgespannte Schrauben haben, werden traditionell in den Stahlkonstruktionen genutzt, welche der zyklischen Belastung. Aus diesem Grund wird die Schiebebelastung über die Reibungsflächen, und nicht über den Kontakt zwischen der Schraubenfläche und des Lochs übertragen. Die Haupteinflussparameter, welche die Widerstandsfähigkeit gegen das Durchrutschen der Verbindung festlegen, sind die Reibung zwischen den Kontaktflächen, sowie die Ebene der Vorspannung in den Schrauben. In dieser Arbeit wurden die Ergebnisse der experimentalen Prüfungen der vorgespannten Schraubenverbindungen unter der zyklischen Belastung dargestellt, mit dem Hauptziel der Prüfung des Einflusses der zyklischen Belastung auf den Verlust der Vorspannkraft in den hochwertigen Schrauben und in den Schrauben für die Verhinderung des Aufdrehens/des Rückwärtsdrehens.

Schlüsselwörter:
hochwertige Schraube, Vorspannkraft, Vorspannverlust, Faktor des Durchrutschens, zyklische Belastung

1. Introduction

Bolted preloaded slip-resistant connections are often used in steel structures when slip between connected members should be restricted. and in cases when the structure is subjected to variable loads or high stress ranges, which may lead to fatigue damage. Bridges, cranes, lattice towers and masts for transmission lines, as well as supporting structures for wind turbines, require strict control of the slipping, and limited deformation in the connection, in order to decrease its negative influence on fatigue resistance and durability, respectively. By preloading the bolts, shear connections, in which the load is transferred by shear of the bolt and pressure applied to the surface of the hole (bearing type), become friction connections. Around the holes, pressure contact areas-resulting from the preload of the bolts-are responsible for transmission of shear load acting by friction.

Main parameters influencing slip resistance of such connections are the value of the slip factor between contact surfaces, the level of preloading in the bolts, and initial imperfections of the connected plates. After clamping of the connected plates, the preloading force can be reduced mainly due to the creep of surface protection, bolt stress relaxation, creep of plates, inadequate corrosion protection, and bolt plasticization in the active thread zone [1]. Besides, the effects of the bolt assembly and bolt type in the connection on the magnitude of the preload loss have also been acknowledged in literature [2]. The preload level decreases over time as a result of coating and bolt creep; hence, it is necessary to assess the preload of the bolts at each time point during service life of a connection in order to predict the total connection lifetime. The preload loss time-term involves the following:

- initial preload loss depending on the bolt installation method
- short-term relaxation, which occurs in the first 12 hours after bolt installation
- long-term relaxation, which is assumed to proceed asymptotically.

The notions of short-term relaxation and long-term relaxation are used in order to distinguish between two inherently different causes for relaxation [3]. The initial preload losses increase with an increase in preload force. The same applies in the case of preloading beyond the yield strength of the bolts [4]. In addition, inadequate quality of the preload process leads to larger initial preload losses, which increase with a decrease in bolt length [5]. If the contact pressure on the contact surface is high enough to cause the corrosion protection layer to creep, a loss of preload will occur in the bolt and, consequently, in the connection as well, leading to a decrease in slip resistance of the connection [6]. So far, research has shown that the total preload loss in high strength bolts is highly dependent on the type and thickness of the corrosion protection applied to friction surfaces[7-9]. The overall thickness of the corrosion protection increases with an increase in the number of plates in the friction connection, leading to lower axial stiffness (Young's modulus) of the materials and, consequently, to a significant loss of preload in high strength bolts [10].

Extensive efforts have been devoted to study the impact of corrosion protection systems on the slip factor and preload loss. In parallel with specimens without corrosion protection (control specimens), most of the research has been performed on specimens with galvanized surfaces [9, 11] and zinc-based metallized coating [12, 13]. Besides, tests on specimens with zinc-silicate coatings have also been carried out [11, 14]. D'Aniello et al. [15] performed monotonic and both variable and constant amplitude cyclic tests on HV and HR bolt assemblies, varying shank diameters (M16, M20 and M24). The monotonic tests enabled identification of failure modes and the force-displacement monotonic response per type of bolt assembly. The variable amplitude cyclic tests enabled assessment of the impact the cyclic actions have on the strength and deformation capacity reduction of bolt assemblies under study, whereas the constant amplitude low-cycle tests enabled identification of fatigue capacities of the bolt assemblies, and determination of the strain-number of cycles curves. Cavallaro et al. [16] experimentally studied variability of preload forces of the bolt assemblies that were used in friction dampers over a period of time. The short-term and mid-term tests indicated that the estimated preload losses after 50 years, in case of assemblies with normal HV washer (EN14399-6) or with disc springs washer (DIN 6796) is, on an average, equal to 10 % and 27 %, respectively. The experimental results also show that, in all cases, the greatest part of the total preload losses, approximately equal to 70 %, occurred in just 30 days. D'Antimo et al. [17] experimentally assessed preload losses in slotted bolted connections under service load conditions, examining the possibility to limit the loss by considering various conical-washer layouts. The results gained through the short-, mid-, and long-term tests were used to calibrate an analytical model that was able to predict the loss of preload over time, accounting for the influence of external loads. It was concluded that the model can reproduce quite accurately the response of bolt connections with various washer layouts, with the maximum error of about 20 % for the configuration with pre-set disk springs. Dongxu et al. [18] performed experiments on 96 high-strength steel bolts of grade 12.9 to quantify ultimate strength capacities under tension and shear, as well as under the combined tension and shear. In addition, the effects of preloading were investigated through several partially threaded bolts. The experimental results were used to assess accuracy of design procedures defined in European and North American specifications, and appropriate modifications were proposed in terms of design equations and reduction factors. Jovanović et al. [19, 20] performed extensive experimental and numerical investigations of structural responses of the end-plate moment connection with four bolts per row. The experimental programme comprised tests on 36 unscaled

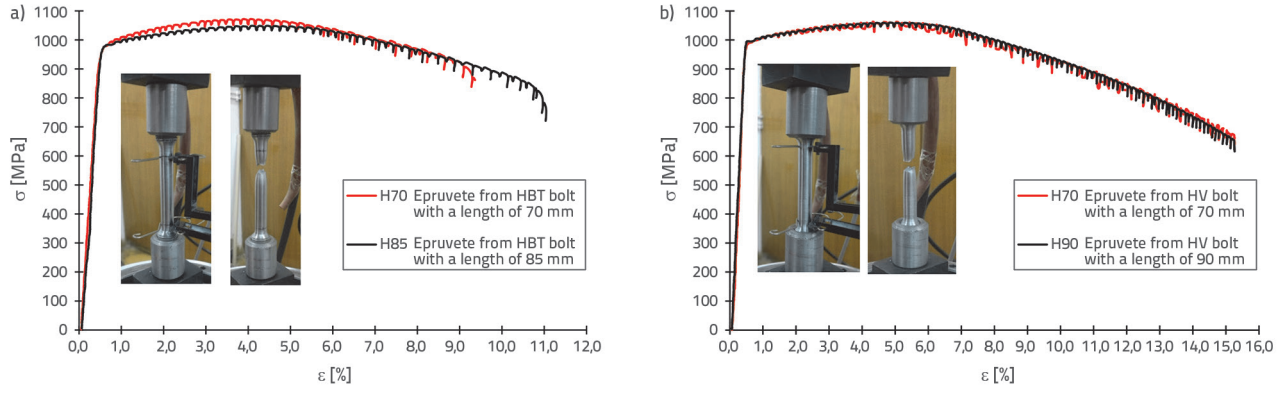

Figure 1. Engineering stress-strain curves: a) HBT bolt test; b) HV bolt test

specimens of T-stub elements and 4 specimens of beam-to-column joints with end-plate connection and four bolts per row. The bolting assemblies of each specimen included strain gauges embedded in bolts aiming to measure the axial strain along the bolt. The preloading behaviour of stainless steel bolted assemblies, and the performance of stainless steel slip resistant connections, were also investigated [21].

This paper presents a part of a comprehensive investigation conducted at the University of Belgrade, Faculty of Civil Engineering, which was carried out to quantify the losses of preloading in high strength bolt (HV) and lockbolt (HBT) slip-resistance connections [22]. The paper addresses an experimental study of preloaded bolted connections exposed to cyclic loading to evaluate the change of preloading after variable (cyclic) actions. The main objectives are to investigate the preloading procedure and to compare the achievable and remaining preloads with regard to the nominal minimum preloading force $F_{p,C}$ of conventional HV bolts and, in parallel, of alternative lockbolts.

The experimental investigation clearly demonstrates that the use of the "Resist 86" zinc-silicate coating on steel plates in slip-resistant shear connections provides Class of friction surface B, according to EN 1993-1-8 [23] ensuring a negligible loss of preload force in the bolts when connections are exposed to cyclic loading involving $2 \cdot 10^6$ cycles.

2. Experimental programme

An experimental program was conceived to determine main parameters influencing behaviour of slip-resistant connections including:

- tensile tests to determine mechanical performance of high strength bolts - HV bolted assemblies according to EN 14399-4 [24] and HBT bolts - alternative high-strength bolting systems for preloading, i.e. Huck BobTail - Lockbolts
- tests to determine the nut factor k for HV bolts and slip factor between friction surfaces of connection plates (specimens with M16 and M20 bolts) on which the zinc-silicate coating was applied
- cyclic loading tests on double lap shear connections to quantify preload loses under cyclic loading.

The test matrix included HV and HBT class 10.9 bolts 20 mm in nominal diameter. The preloading in the bolts was measured employing instrumented bolts with implanted strain gauges.

2.1. Material tests

Two machined tension specimens were made from HV and HBT bolts according to EN ISO 898-1 [25] to measure mechanical properties. Displacement-controlled tensile tests were performed in accordance with requirements specified in EN ISO 6892-1 [26]. The tests were carried out on an AG-Xplus Universal Testing Machine (Shimadzu, Japan) with a capacity of 300 kN. The calibrated extensometer with a gauge length, L_0, of 50 mm was used to measure longitudinal strain of test coupons. The adopted test speed was 0.1 mm/min for the initial part of the test, i.e. up to approximately 1 % of total strain, after which the speed was increased to 2.0 mm/min.

The obtained engineering stress–strain curves, along with the tensile coupon test setup, are provided in Figure 1 for both HBT and HV bolts. The experimental results confirmed the nominal steel grade of the bolts. The mean values of yield strength, f_y, for HBT and HV bolts are 976 N/mm^2 and 993 N/mm^2, respectively. whereas the mean values of ultimate tensile strength, f_u, for HBT and HV bolts are 1060.4 N/mm^2 and 1061.6 N/mm^2, respectively.

2.2. Determination of friction coefficient between nut thread and bolt shank of HV bolts

Friction tests were based on standard tests from EN1090-2 [27]. The friction coefficient between the nut thread and bolt shank of HV bolts was measured on nine zinc-coated HV bolts 20 mm in nominal diameter. The bolts had a protective layer with thicknesses ranging from 45 μm to 90 μm. Four bolts 70 mm in length and five bolts 90 mm in length were used from the same batch. During the bolt installation into the calibration equipment,

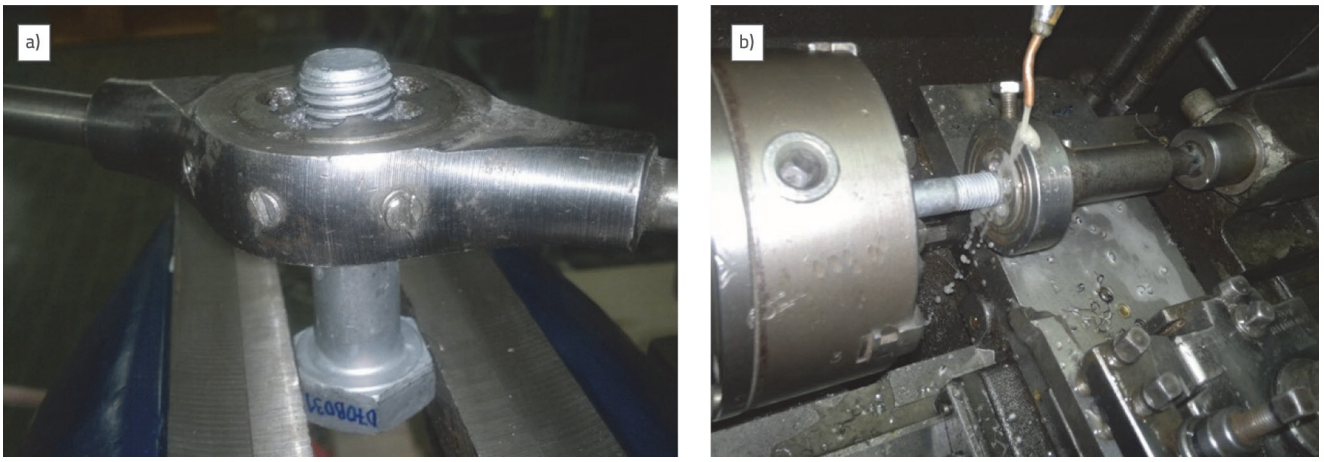

Figure 2. Removal of zinc from bolt thread: a) Removal of zinc by die; b) Removal of zinc by lathe machine

it was observed that a significant number of bolts could not be installed into the metric thread. Therefore, the threads of each bolt were processed ("cleaned") with a die or by a lathe machine, as shown in Figure 2a and Figure 2b, respectively. The excess zinc was removed from the thread, enabling easy installation into the calibration equipment. It is important to note that the coefficient μ was determined on bolts whose threads were processed as described above. The tests were performed according to EN 1993-1-8 [23] and EN ISO 16047 [28] using the following equipment:

- moment scale Torqueleader, model N 2000, range 100–2000 Nm
- tensometer Stahlwille, range up to 300 kN
- wrench Rahsol DremoMeter type D, range 140–760 Nm.

Table 1 lists the measured tightening torques $T_{Fp,C}$, bolt preload forces $F_{p,C}$ and friction coefficient between nut thread and bolt shank (k – factor). The average value of the k - factor is 0.143 with a coefficient of variation (CoV) of 7.4 %.

2.3. Slip factor determination

The slip factor between connected steel plates protected by the "Resist 86" zinc-silicate coating was determined according to EN 1090-2 [27]. The test procedure was conducted on the double lap shear connections with steel plates whose friction surfaces were prepared according to the treatment being tested, and then loaded in tension.

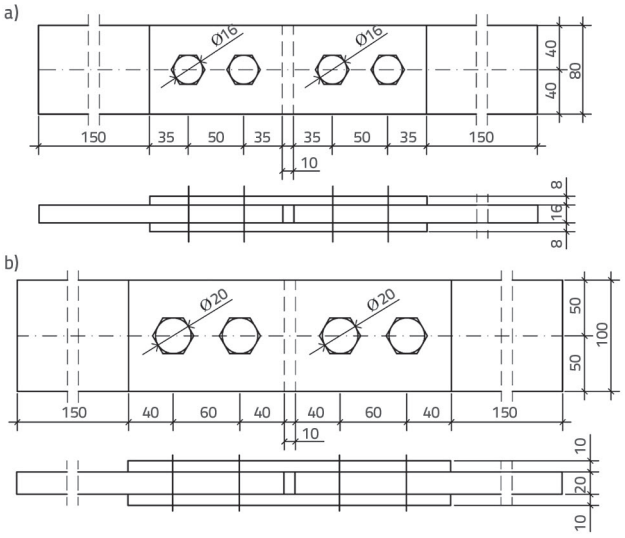

Figure 3. Nominal geometry of specimens used to measure slip factor between connected plates: a) specimen plates with HV bolts M16; b) specimen plates with HV bolts M20 (all dimensions are in mm)

Table 1. Results of tests for friction coefficient between nut thread and bolt shank of HV bolts

No. of bolt specimen	Bolt	$T_{Fp,C}$ [Nm]	$F_{p,C}$ [kN]	k	k_{mean}	CoV [%]
1	M20x70	500	164	0.152	0.143	7.4
2	M20x70	470	180	0.131		
3	M20x70	445	168	0.132		
4	M20x70	435	160	0.136		
5	M20x90	480	150	0.160		
6	M20x90	480	162	0.148		
7	M20x90	435	150	0.145		
8	M20x90	450	147	0.153		
9	M20x90	450	169	0.133		

One test series comprised six specimens. Three specimens were tightened with HV bolts M16 and three with HV bolts M20. Each specimen includes four bolts. The geometry of the specimens is in accordance with Annex G, EN 1090-2 [27]. In all tested specimens, the hole geometry corresponded to normal circular holes. Nominal geometry of specimens used in the tests is depicted in Figure 3. The steel grade of connected plates was S355JRG2.

The specimen designation "F-X-M16 (or M20)" provides the following information: the first letter F indicates friction test; the second numeral X represents the ordinal number of specimens, whereas the ensuing alphanumeric designation M16 and M20 is nominal designation of the bolt.

The preparation of specimens was done by sandblasting to the preparation grade Sa 2.5 according to EN ISO 8501-1 [29], using the "Medium G" abrasive 30–50 μm in diameter. After cleaning the specimens, the "Resist 86" coating was applied on dry surface by brush in two layers. The average dry (coating) film thicknesses measured with laboratory elcometer at characteristic points, were as follows:

- 88.4 μm for specimens with 16-mm diameter holes (film thickness ranging from 65.4 to 110 μm) measured 24 h after application of the coating;
- 91.8 μm for coupons with 20-mm diameter holes (film thickness ranging from 60.5 to 124 μm), measured 24 h after application of the coating.

Ambient conditions were measured throughout the surface preparation procedures, Table 2.

Table 2. Ambient conditions during coating application

Air temperature [°C]	Surface temperature [°C]	Dew point [°C]	Relative humidity [%]
19.2	17.5	14.7	76.0

High strength bolts were installed in the specimens in a package: bolt, nut, and two washers. Tightening was done using a calibrated wrench ("RAHSOL", type D, with a 280–760 Nm range) by determining the preload, which was applied to each bolt by a tightening torque.

The testing was performed on an 800-kN capacity test rig in tension with "SCAIME CA40X40t C4 CH 10e" force convertors. The HV bolts used in this test remained in the elastic range after installation, and consequently, could be preloaded multiple times. Before installation, the bolts were preloaded on the tensometer using a calibrated wrench. The controlled applied force achieved during the installation was determined in this way. The following step was to install the bolts into specimens and determine the slip factor. At the end, the same bolts were preloaded again, controlled by the tensometer using a calibrated wrench which was the basis for determining the preload force. When calculating the slip factor, average values of these two preload measurements were taken. The total preload represents the sum of the bolt preload on each side of the connection. Before testing, two dial gauges were attached at both sides of the connection. Thus, the displacement of points A and C, relative to point B, was measured, and forces at which slip occurred were registered. The force level at which displacement of points A and C, relative to point B, greater than δ = 150 μm occurred, was adopted as the slip force. The test setup for determining the friction force is shown in Figure 4.

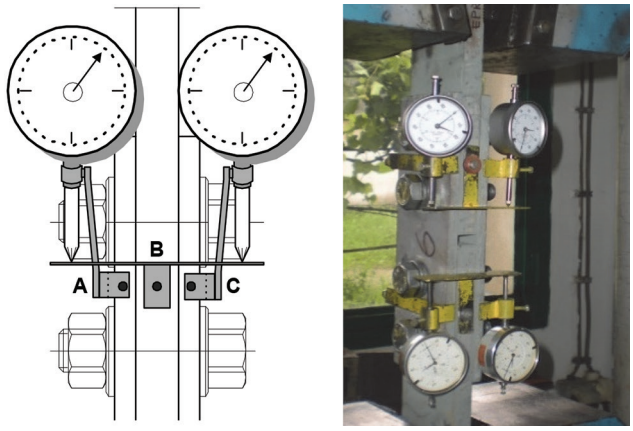

Figure 4. Test setup for friction force measurements

The test schedule was adapted to a scenario involving construction of a new steel structure. In such a case, the corrosion protection of steel members is applied before they are erected, and a significant time can elapse between application of the coating and member erection. Therefore, the coating was applied to the specimens 10 days prior to preloading of the bolts, and the specimens were tested 24 h after the bolts were preloaded. The following notation, shown in Figure 5, was adopted for the presentation and analysis of results: F_{pt1}, F_{pt2} are the bolt preload forces at specimen top surface, F_{pb1}, F_{pb2} are the bolt preload forces at specimen bottom surface, F_{tt1} is the slip force at specimen top side, and F_{tb1} is the slip force at specimen bottom side.

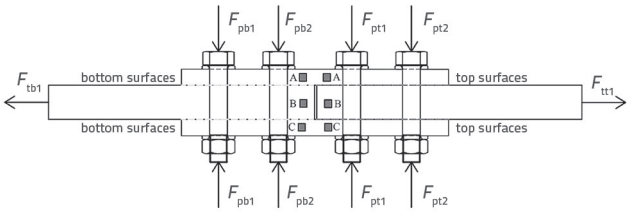

Figure 5. Labelling of forces acting on specimens and tensometer measurement positions

Key experimental results are summarised in Table 3 and Table 4 for specimens with bolts M16 and M20, respectively, considering the top and bottom friction surfaces, in which DFT is dry film thickness.

Although creep tests (in accordance with EN 1090-2 [27]) were not performed, the obtained results clearly indicate that when the coating "Resist 86" was used, the connection with Class of friction surface B, in accordance with EN 1993-1-8 [23], was achieved, even in the worst-case scenario.

Table 3. Results of tests for slip factor between connected plates for specimens with M16 bolts

Specimens	Friction surface	DFT [μm]	Bolt forces F_{pt} & F_{pb} [kN]		Total preload force $F_{p.c}$ [kN]	Slip force F_t [kN]	Slip factor μ
F1M16	Top surfaces	88.4	F_{pt1} = 100	F_{pt2} = 100	200	203.8	0.51
	Bottom surfaces	88.4	F_{pb1} = 103	F_{pb2} = 107	210	203.8	0.48
F2M16	Top surfaces	88.4	F_{pt1} = 107	F_{pt2} = 107	214	208.2	0.49
	Bottom surfaces	88.4	F_{pb1} = 108	F_{pb2} = 115	223	208.2	0.47
F3M16	Top surfaces	88.4	F_{pt1} = 92	F_{pt2} = 93	185	190.1	0.51
	Bottom surfaces	88.4	F_{pb1} = 91	F_{pb2} = 90	181	190.1	0.52
Mean value							0.50
Standard deviation							0.0197
Coefficient of variation [%]							3.90

Table 4. Results of tests for slip factor between connected plates for specimens with M20 bolts

Specimens	Friction surface	DFT [μm]	Bolt forces F_{pt} & F_{pb} [kN]		Total preload force $F_{p.c}$ [kN]	Slip force F_t [kN]	Slip factor μ
F1M20	Top surfaces	91.8	F_{pt1} = 160	F_{pt2} = 170	330	324.6	0.49
	Bottom surfaces	91.8	F_{pb1} = 164	F_{pb2} = 163	327	324.6	0.50
F2M20	Top surfaces	91.8	F_{pt1} = 160	F_{pt2} = 154	314	285.2	0.45
	Bottom surfaces	91.8	F_{pb1} = 152	F_{pb2} = 145	297	285.2	0.48
F3M20	Top surfaces	91.8	F_{pt1} = 162	F_{pt2} = 170	332	306.8	0.46
	Bottom surfaces	91.8	F_{pb1} = 177	F_{pb2} = 155	332	306.8	0.46
Mean value							0.47
Standard deviation							0.0197
Coefficient of variation [%]							4.20

Figure 6. Specimens tightened with M16 bolts after testing

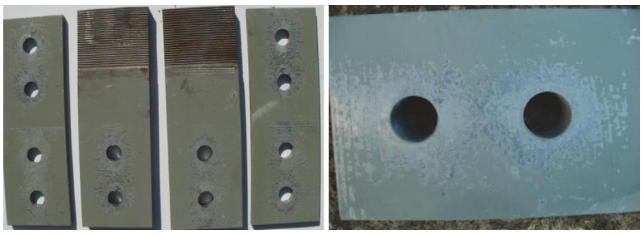

Figure 7. Specimens tightened with M20 bolts after testing

Figure 6 and Figure 7 show visible active friction zones of connected plates around the bolts for specimens with preloaded bolts M16 and M20, respectively. There is no damage of the base material around the holes for the connecting devices, indicating that the bolts were not under bending during the testing.

2.4. Preload measurement

The preload in bolting assemblies during relaxation tests and tests under cyclic load was measured using implanted strain gauges. The method is based on measuring axial strain along the bolt via a strain gauge, which is usually embedded in a bolt, and by performing calibration through comparison of readings with load cell measurements. The relationship between the strain measurements and force levels depends on the scatter of the modulus of elasticity E and effective area A of the bolts where strain gauge is embedded (which also depends on the position of strain gauges in the bolt). The scatter of E and A is experimentally established by calibration to provide for the strain level that ensures a required preload force in a bolt. The procedure for installing the strain gauge into the bolt involves special thermal treatments of the bolts to achieve glue hardening.

Table 5. "BTM-6C" strain gauge properties

Strain gauge type	Strain gauge [mm]		Strain gauge carrier [mm]		Strain gauge center [mm]		Resistance [Ω]	Hole diameter [mm]
	Length L_{sg}	Width d_{sg}	Length L	Width d	a	b		
BTM – 6C	6	1,0	12,0	1,7	5	7	120	Ø 2,0

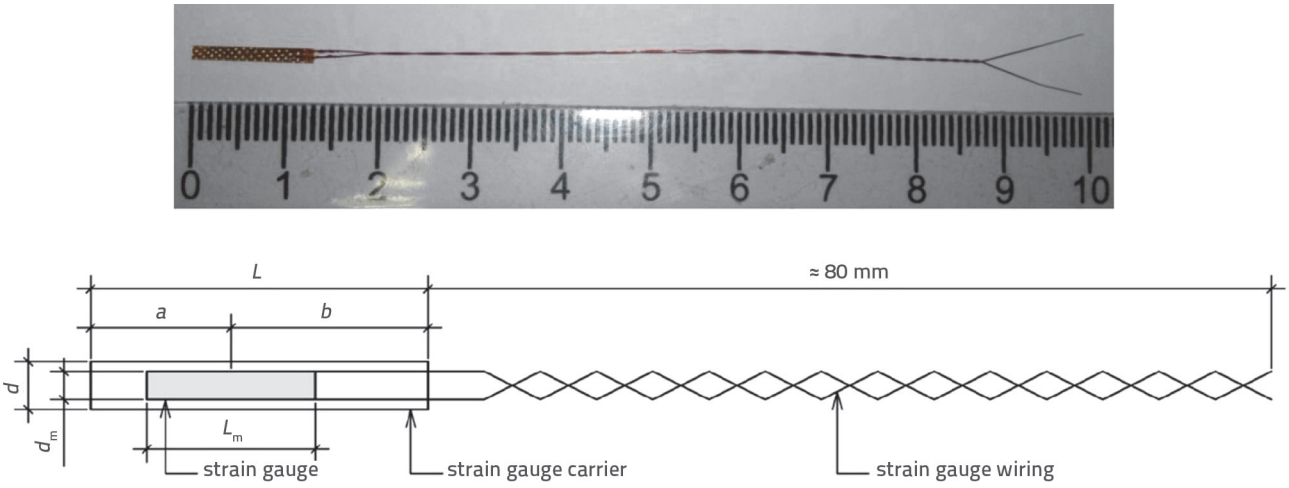

Figure 8. BTM-6C strain gauge

The BTM-6C (Tokyo Sokki Kenkyujo Co, Japan) strain gauges were used for measuring the value and variation of preload in bolts (see Table 5).

According to the specification list, the strain gauges may be used in the temperature range from –10°C to +80°C, and their measurement range is $5000 \cdot 10^{-6}$ μm/m. The strain gauge wiring consisted of copper wires with a polyurethane insulation, with a diameter of 0.14 mm and an approximate length of 80 mm, see Figure 8.

The strain gauges were embedded into Ø2 mm holes drilled in the bolt axis. The inside of the hole, the bolt head, and the shank, were cleaned using a solvent to remove any remaining dust or splinters. The strain gauges were positioned in the zone in which the variation of the bolt cross-section area is minimal (the shank section outside the threaded region). This requirement cannot be fulfilled in the case of HBT bolts since the thread runs across the entire shank. In this case, the strain gauge centre should be in the middle of the clamping zone after installation. The most efficient way to embed a strain gauge into the desired position is to mark the strain gauge carrier accordingly. On the marked spots, the strain gauge carrier is bent at right angle, taking care not to damage the insulation; the obtained strain gauge shape ensures that it will be embedded appropriately. The positioning of the strain gauge in HV bolts with a length of 50 mm, and embedding of a rectangular bended strain gauge into bolts, are presented in Figure 9.

The adhesive used for fixing the BTM-6C strain gauge carries the manufacturer's label "A-2". Before embedding the strain gauge, the same glue that was injected into the bolt hole also needs to be applied onto the strain gauge itself. After that, the strain gauge is embedded into the bolt shank in such a way that the bent part of the wire connected to the strain-gauge carrier sits on the bolt head. The strain gauge should be embedded vertically, and aligned with the hole axis. After fixing the position of the strain gauge, bolts are exposed to thermal treatment of glue in a laboratory dryer with a thermal probe-controlled temperature regime. After hardening of the glue and subsequent cooling of the bolts, the strain gauge wiring can be connected to the data acquisition system to check functioning of the strain gauge.

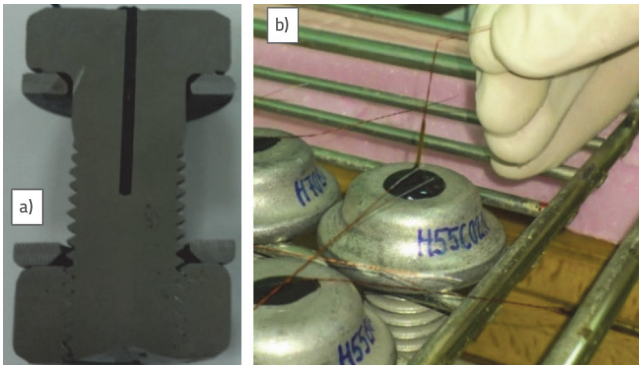

Figure 9. a) Positioning strain gauge in HV bolt; b) embedding rectangular bended strain gauge into HBT bolts

The very sensitive wiring of strain gauges requires adequate protection against damage or tear during testing. For this reason, two pertinax plates are glued to the bolt head and the wiring is soldered to them as are the cables connecting the strain gauge to the data acquisition system. The wiring is protected by a two-component glue and silicone, see Figure 10. To compensate for temperature effects, a compensatory strain gauge was glued to a steel plate for each strain gauge embedded in a bolt, see Figure 11.

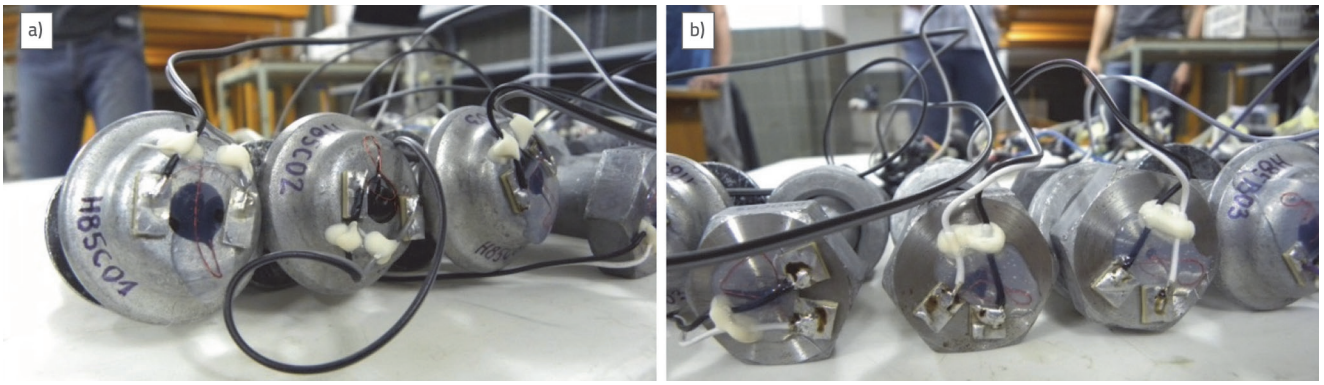

Figure 10. Protection of strain gauge wiring

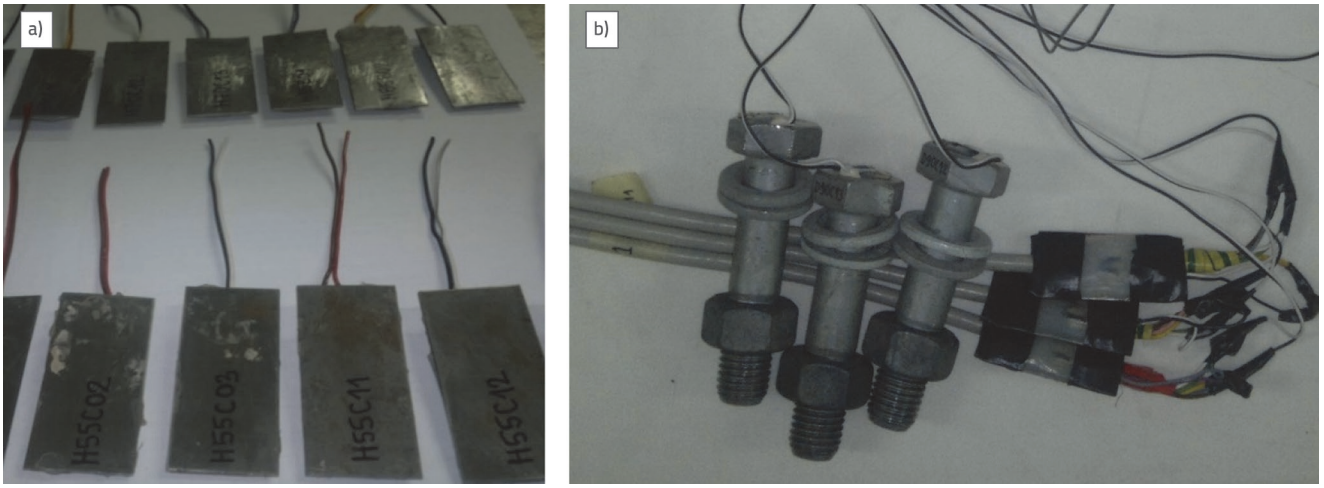

Figure 11. Compensatory strain gauges

The calibration procedure was carried out using a 400 kN capacity Schenk testing machine. A special device was constructed allowing the operator to fix the bolt in the testing machine and the load is measured at a predefined load level.

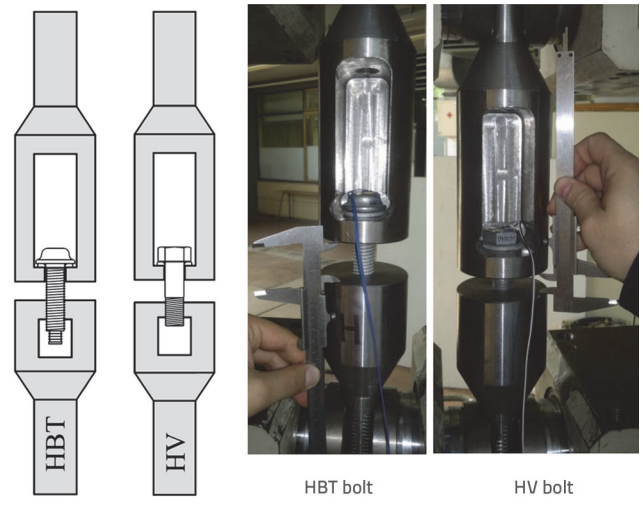

Figure 12. Test layout for bolt calibration

The device was constructed based on the geometry of the testing machine jaw and the HBT and HV tested bolts. Figure 12 shows a test layout for bolt calibration.

A labelling method ensuring that each bolt has a unique label was adopted, as shown in Table 5. The first letter indicates bolt type, i.e. D - HV bolts according to EN 14399-4 [30] and, H - Huck BobTail bolts. The number in the second and third positions (50, 55, 70, 85, 90) stands for the bolt shank length. The subsequent letter C indicates that bolts are installed in specimens whose surfaces are coated with corrosion protection (coating). The numeral in the fifth position signifies that the specimens are exposed to cyclic loading. In order to study the effect of preloading of one bolt on an adjacent already preloaded bolt, a controlled installation sequence was performed. Thus, the labelling of bolts included a numeral in the sixth position that indicates the bolt installation order. In the connection label (main tests on preload loss under cyclic loading), the first letter indicates the type of installed bolts whereas the numeral in the second position represents the ordinal number of the specimen (see Table 6).

Table 6. Labelling system of connections and installed bolts exposed to cyclic load

Bolt label	Connection label	Bolt label	Connection label
D50C11	D3	H55C11	H3
D50C12		H55C12	
D50C13		H55C13	
D70C11	D6	H70C11	H6
D70C12		H70C12	
D70C13		H70C13	
D90C11	D9	H85C11	H9
D90C12		H85C12	
D90C13		H85C13	

The test procedure described in [2] was adopted. The procedure involves gradual application of the load with at least three loading-unloading cycles; after the first loading the load level was maintained at its maximum value for 300 s, whereas in all other cases it was maintained at the maximum or minimum value for 30 s, see Figure 13.

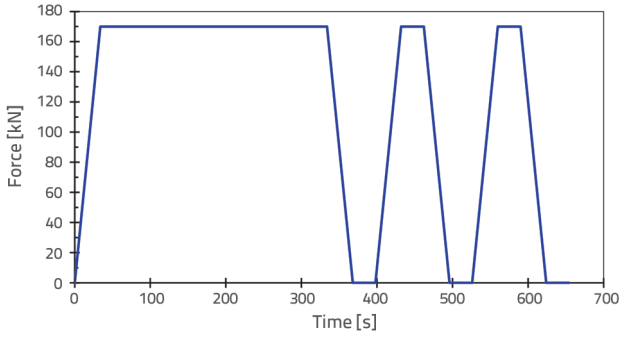

Figure 13. Force-Time diagram on the testing machine during bolt calibration [2]

Maintaining the force level for 300 s after the first cycle enables control of the strain gauge's functioning through the stability of the readings. If a "slip" of the strain gauge occurs (a drop in strain at constant force), it is a sure indicator that the strain gauge is not embedded properly. The loading and unloading speeds were always maintained at 5 kN/s. The maximum tensile force used to load the bolts during calibration was chosen so as to be close to the expected preload force, but also uniform for all bolts. The fear of damaging bolt threads during calibration [31] is certainly unjustified. Throughout the calibration process, readings from the strain gauges were taken at 5 Hz. If the result was a linear relation between the force acting on the bolt and the strain measured by strain gauge (over the entire load range and in all loading-unloading cycles), the strain gauge was deemed to function properly, and the bolt was considered ready for installation.

In this type of experimental investigation, a total of 18 bolts were calibrated and the relation between the applied force and strain measured by the strain gauge was determined for each bolt. From the obtained results, the stress–strain relationship was determined using the least squares method. In this way, the behaviour of every bolt was known from the calibration curve and correlation coefficient. Three distinct calibration curve types were observed:

- a perfect linear relation between force and strain, Figure 14a
- curves with a certain nonlinearity at smaller forces, Figure 14b
- curves displaying a hysteretic behaviour (causing these bolts to be rejected from use in experiments), Figure 14c.

The linear relation between the applied force and strain measured by the strain gauge is a proof of correct strain gauge embedment in the bolt, and of proper gluing action, enabling the strain gauge to follow the bolt behaviour (matching of bolt strains in the strain gauge zone with strains in the strain gauge). At the same time, the strain level from strain gauges is linked to the force level. As an example, the calibration curve for bolt H70C11, along with the equation obtained using the least squares method and the coefficients of correlation, is shown in Figure 14.

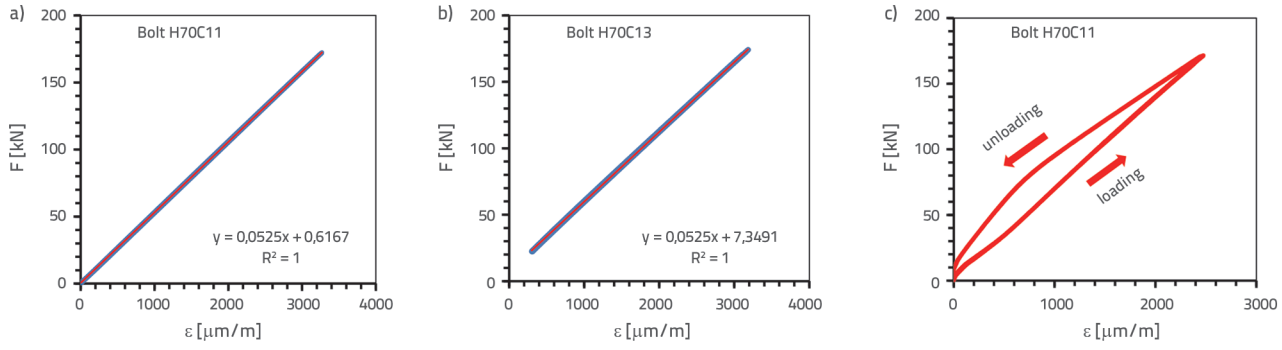

Figure 14. Force–displacement diagrams: a) calibrated bolt H70C11 linear relation between force and strain; b) calibrated bolt H70C13 curve with a certain nonlinearity at smaller forces; c) calibrated bolt H70C11incorrectly installed strain gauge

2.5. Tests on preload loss exposed to cyclic loading

Cyclic tests were performed on six specimens - three HV bolts and three HBT bolts. Each specimen consisted of three steel plates and three bolts forming together a double lap connection. All bolts had a nominal diameter of 20 mm. HV bolts were used in the lengths of 50, 70, and 90 mm, whereas the lengths of HBT bolts were 55, 70, and 85 mm. For the specimens, three package thicknesses consisting of thicknesses of individual plates, were selected: $t_{1,1} + t_{2,1} + t_{1,1} = 5 + 8 + 5 = 18$ mm, $t_{1,2} + t_{2,2} + t_{1,2} = 10 + 15 + 10 = 35$ mm, and $t_{1,3} + t_{2,3} + t_{1,3} = 15 + 25 + 15 = 55$ mm. All specimens were cut from a steel plate class S355JRG2. Sandblasting was performed in an automatic machine using quartz sand as the abrasive. Dust was removed from cleaned surfaces using a jet of compressed air and brushes. In this way, the surfaces were prepared for corrosion protection using zinc-silicate coatings. The geometries of the tested specimens with HV and HBT bolts are shown in Figure 15a and Figure 15b, respectively.

Bolts were installed and specimen were formed in the Laboratory for concrete and rheology of the Faculty of Civil Engineering - University of Belgrade.

Available standards prescribe minimum preload force values for high strength bolts:

- for M20 HV bolts, according to EN 1993-1-8 [23] $F_{p,C} = 171.5$ kN,
- for M20 HBT bolts, according to the draft standard [32] $F_{p,C} = 170.7$ kN.

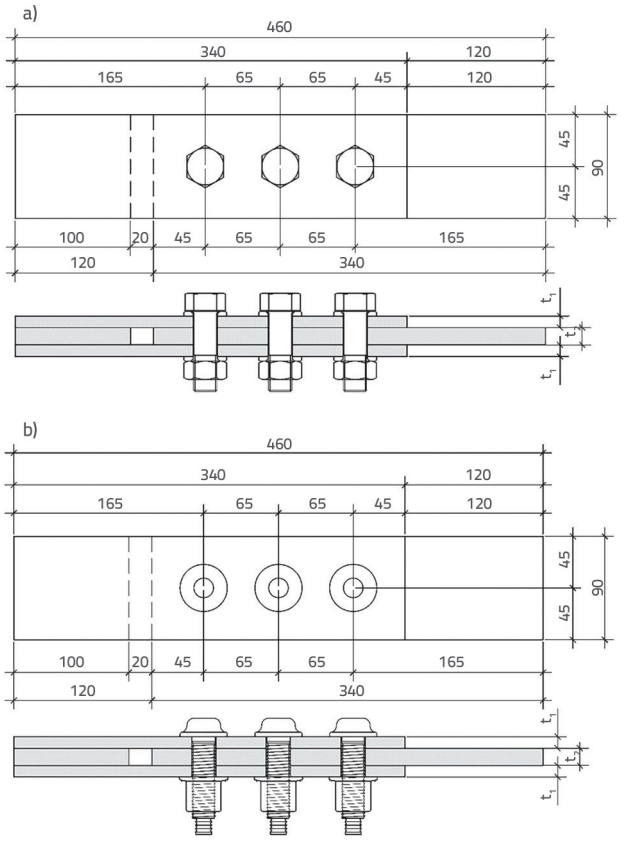

Figure 15. Nominal geometry of specimens with HBT bolts: a) Specimens with HV bolts; b) Specimens with HBT bolts (all dimensions are in mm)

Installation of HV bolts using a calibrated wrench is defined by EN 1090-2 [27]. The installation (torque method) is carried out in two steps. First, the bolts are preloaded to 75 % of the tightening torque determined from the prescribed force value $F_{p,C}$. After doing this for all bolts in the connection, they are preloaded in the second step to 110 % of the same tightening torque, which is at the same time the end of their installation.

In this experiment, HV bolts were preloaded in one step, up to the full tightening torque value. It was estimated that this would enable better perception of targeted phenomena and easier comparison of results with those for HBT bolts.

Because of highly specific specimens, it was necessary to devise an adequate way for installing the HV bolts. Since they are

Figure 16. Bolt installation in specimens

installed using a calibrated or ordinary wrench, the bolt heads had to be fixed using a parallel-table vice clamp, Figure 16. This proved to be a good solution and enabled quick installation of the bolts.

No special conditions were necessary for installation of "Huck BobTail" bolts, given the way the hydraulic press for installation operates. Their installation fully confirmed the specified speed of 2 s per bolt as well as the simple and intuitive procedure that does not require specifically skilled labour.

The specimens were exposed to cyclic loading after one month of monitoring of the initial and short-term preload losses. The experiment was conducted on an MTS testing machine with a capacity of ±500 kN. The cyclic loading was applied in 105 cycles with a 700 seconds pause after each series in order to monitor the bolt preload forces. The pause served to stabilize the specimen and the preload force.

In each cycle, the load spectrum was defined by frequency and minimal and maximal forces F_{min} and F_{max}, respectively, see Figure 17. When determining the cyclic force range, the aim was to simulate service load of a structure designed for the fatigue load at which no slip at the connection should occur during its service lifetime. According to EN 1993-1-9 [33], the double lap connection with preloaded high strength bolts belongs to the detail category 112 where $\Delta\sigma_c$ = 112 MPa is meant for a gross cross-section area of the connecting plate. Hence, if this connection is loaded cyclically causing a stress range of $\Delta\sigma_c$ = 112 MPa in the steel plates' gross cross-section, fatigue failure will occur after $2{\cdot}10^6$ cycles. In the experiment, the cyclic force range (difference between maximal and minimal cyclic force in each cycle) was determined so that the limiting stress range in the specimen corresponds to 75 % of the value defined as the limit for this detail class – $\Delta\sigma_c$ = 112 MPa.

Two extensometers were installed on each specimen in order to register potential slip between plates. A special device, specifically designed for the installation of these extensometers, was temporarily glued to the side of the steel plates, and it enabled monitoring of any differential movement between the steel plates. HBM's DD1-type extensometer was used. Its measurement range is ±2.5 mm and its precision of 0.5 % (0.0125 mm) of the measurement range is sufficient to register differential movement of the steel plates larger than 0.15 mm, which was the slip criterion.

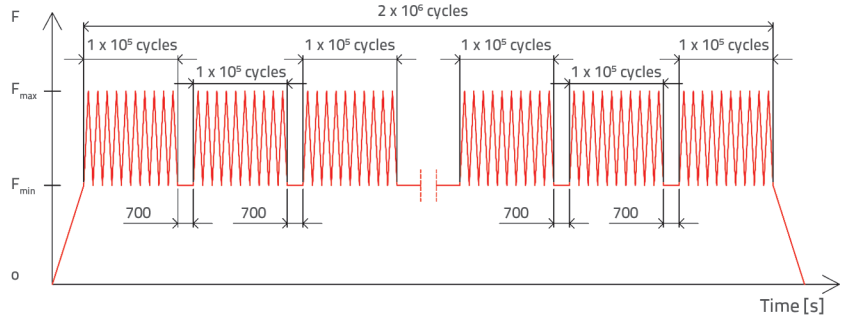

Figure 17. Cyclic loading spectrum in experiment

Immediately prior to placing the specimens in the testing machine for cyclic loading, strain readings were made on strain gauges embedded in bolts and the preload force F_p was calculated in each bolt as follows:

$$F_p = a \cdot x(t_d) + b \tag{1}$$

where, a and b are the bolt calibration curve coefficients, $x(t_d)$ is the embedded strain gauge strain at the beginning of cyclic load testing, and td is the moment in which the cyclic load testing starts.

Based on the calculated preload force values, the bolts' slip resistance, $F_{s,Rd}^{b}$ is determined in accordance with Eq. (2):

$$F_{s,Rd}^{b} = \frac{k_s \cdot n \cdot \mu}{\gamma_{M3}} \cdot F_p \tag{2}$$

where, k_s = 1.0 is the coefficient for bolts in normal holes, n = 2.0 is the number of friction surfaces, μ = 0.45 is the estimated value of slip factor, and γ_{M3} = 1.25 is the partial safety factor.

The specimen slip resistance, $F_{s,Rd}^{b}$ is determined by summing slip resistances of individual bolts:

$$F_{s,Rd}^{s} = \sum F_{s,Rd}^{b} \tag{3}$$

Based on the specimen's cross-section and material strength class, the net section resistance is taken to be the smaller of two values:

$$F_p = a \cdot x(t_d) + b \tag{4}$$

where, A is the specimen gross cross-section area, A_{net} is the specimen net cross-section area, f_y is the material yield strength, f_u is the material ultimate tensile strength, γ_{M0} = 1.0 is the partial safety factor, and γ_{M2} = 1.25 is the partial safety factor.

The maximum and minimum cyclic forces should be adopted, in addition to frequency, in order to completely define the cyclic loading spectrum. One constraint is that no slip should occur during the testing. Hence, the maximum cyclic force value was defined as 80 % of the specimen's slip resistance, as follows:

$$F_{d,max,1} = 0.8 \cdot F_{s,Rd}^{s} \tag{5}$$

An exception to this rule were the thinnest specimens, D3 and H3, where the net section resistance was governing. The maximum value of the cyclic force was defined as 80 % of the specimen's net section resistance, in order to avoid failure of the net section during testing:

$$F_{d,max,2} = 0{,}8 \cdot N_{t,Rd} \tag{6}$$

Table 7. Cyclic load spectrum parameters

Specimen label	Bolt label	F_p [kN]	$F_{bs.Rd}$ [kN]	$F_{ss.Rd}$ [kN]	$N_{t.Rd}$ [kN]	ΔF_d [kN]	$F_{d.max}$ [kN]	$F_{d.min}$ [kN]
D3	D50C11	160.5	115.6	354.8	202.7	60	160	100
	D50C12	165.7	119.3					
	D50C13	166.6	119.9					
H3	H55C11	112.9	81.3	248.8	202.7	60	160	100
	H55C12	107.4	77.3					
	H55C13	125.3	90.2					
D6	D70C11	155.0	111.6	290.7	381.1	110	230	120
	D70C12	137.5	96.7					
	D70C13	118.5	82.4					
H6	H70C11	165.7	119.3	347.0	381.1	110	310	200
	H70C12	141.5	101.9					
	H70C13	174.7	125.8					
D9	D90C11	144.5	104.0	336.6	633.4	190	270	80
	D90C12	132.8	95.6					
	D90C13	190.3	137.0					
H9	H85C11	178.9	128.8	392.4	633.4	190	310	120
	H85C12	195.6	140.8					
	H85C13	170.6	122.8					

Another constraint was the requirement that the fatigue failure of specimens must not occur during cyclic loading. This constraint was taken into account by limiting the specimen stress variation to 75 % of the value defined as the limit for this detail class, i.e., of $\Delta\sigma_c$ = 112 MPa:

$$\Delta F_d = 0{,}75 \cdot \Delta\sigma_c \cdot A \quad (7)$$

Based on the presented constraints, the minimum cyclic force was:

$$F_{d,min} = F_{d,max} - \Delta F_d \quad (8)$$

The cyclic loading limit values obtained in this way were, for practical reasons, rounded to the nearest 10 kN. The cyclic load spectrum for each specimen is presented in Table 7.

3. Experimental results and discussion

Three reference time points were selected for the initial and short-term losses of preload: t_1 is the time when the maximum preload in the bolt shank is reached; this is the time from which the loss of preload is measured. The time t_3 = 10 s is the time when the initial loss of preload is considered to have ended. The time t_4 = 12 h is the time when short-term loss of preload is considered to have ended. Additionally, the time t_2 = 2 s was introduced for HBT bolts indicating the time when the hydraulic press is removed from the bolt tail.

Graphical presentations of initial and short-term losses of preload force $F_{p,C}$ for HV and HBT are shown in Figure 18 and Figure 19, respectively.

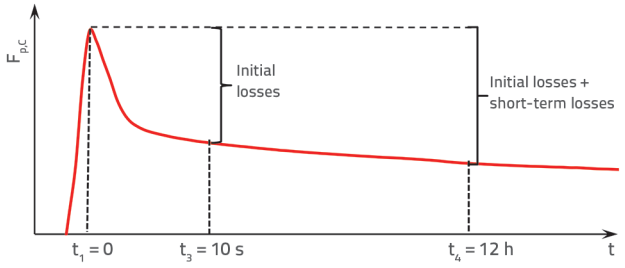

Figure 18. Initial and short-term loss of preload in HV bolts

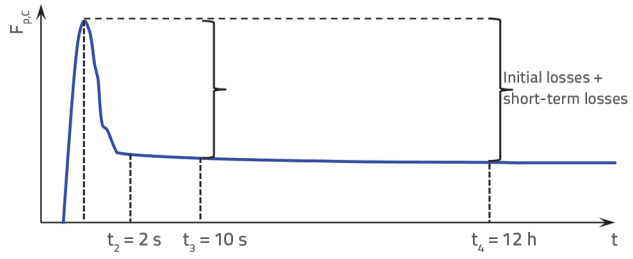

Figure 19. Initial and short-term loss of preload in HBT bolts

The results for HV and HBT bolts considering each reference time point are respectively tabulated in Table 8 and Table 9, where $F_{p,C,max}$ is the maximum high strength bolt preload achieved during installation; $F_{p,C,ti}$ is the bolt preload measured in

Table 8. Initial and short-term losses of preload force in HV bolts

Specimen label / installation method	Bolt label	$F_{p.C.max}$ [kN]	$F_{p.C.t3}$ [kN]	$F_{p.C.t4}$ [kN]	$\Delta F_{p.C.t3}$ [%]	$\Delta F_{p.C.t4}$ [%]
			t_3 = 10 s	t_4 = 12 h		
D3 Calibrated wrench	D50C11	205.2	194.5	170.3	5.20	16.98
	D50C12	199.9	188.7	173.7	5.62	13.12
	D50C13	202.9	192.8	176.5	4.99	13.02
D6 Calibrated wrench	D70C11	194.3	187.1	174.1	3.70	10.41
	D70C12	193.0	183.6	169.3	4.84	12.28
	D70C13	185.7	179.5	166.1	3.38	10.55
D9 Calibrated wrench	D90C11	171.5	163.6	151.9	4.62	11.45
	D90C12	158.9	151.5	139.4	4.63	12.26
	D90C13	232.4	216.3	199.1	6.90	14.32

Table 9. Initial and short-term losses of preload force in HBT bolts

Specimen label	Bolt label	$F_{p.C.max}$ [kN]	$F_{p.C.t2}$ [kN]	$F_{p.C.t3}$ [kN]	$F_{p.C.t4}$ [kN]	$\Delta F_{p.C.t2}$ [%]	$\Delta F_{p.C.t3}$ [%]	$\Delta F_{p.C.t4}$ [%]
			t_2 = 2 s	t_3 = 10 s	t_4 = 12 h			
H3	H55C11	223.8	135.4	131.7	120.7	39.50	41.15	46.07
H3	H55C12	223.1	128.6	124.7	113.5	42.36	44.11	49.11
H3	H55C13	240.6	146.1	141.9	131.4	39.28	41.02	45.37
H6	H70C11	246.1	188.8	179.8	171.9	23.28	26.94	30.14
H6	H70C12	218.1	159.0	156.3	147.2	27.10	28.34	32.50
H6	H70C13	247.3	194.1	191.4	182.4	21.51	22.60	26.24
H9	H85C11	240.0	194.5	192.3	183.9	18.96	19.88	23.36
H9	H85C12	240.6	190.6	188.4	185.1	20.78	21.70	23.06
H9	H85C13	233.9	186.4	184.4	176.1	20.31	21.16	24.71

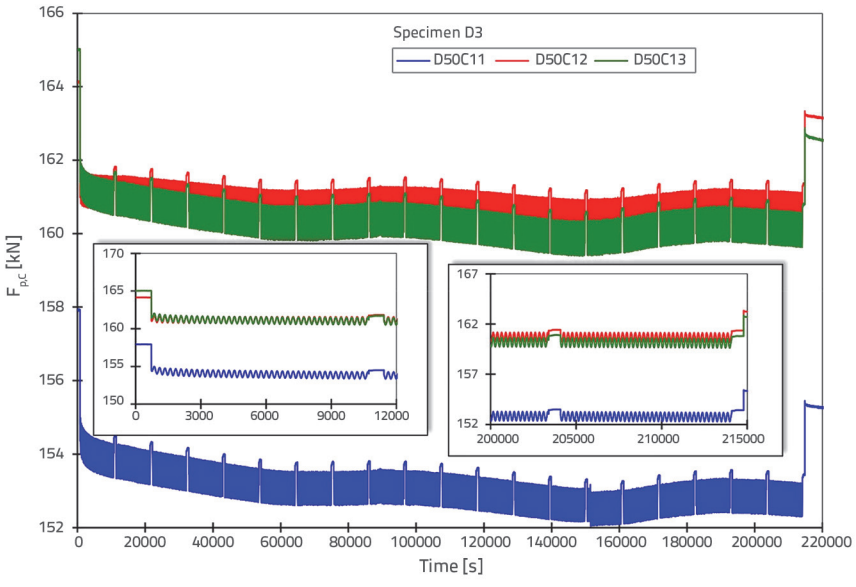

Figure 20. Change of preload in specimen D3 bolts during cyclic loading

the time t_i after achieving the maximum preload; $\Delta F_{p,C,ti}$ is the loss of preload in the time t_i after achieving the maximum preload value.

Besides, as an example, the change of preload for specimen D3 exposed to cyclic loading is shown in Figure 20. The enlarged sections of the diagrams clearly display the beginning and end of the cyclic test and the preload value before and after the cyclic loading.

Key experimental results associated with cycle load testing are respectively listed in Table 10 and Table 11 for HV and HBT bolts, where: $F_{p,C,d1}$ is the preload force in the bolt before the start of the cyclic load test; $F_{p,C,d2}$ is the preload force in the bolt at the end of the cyclic load test; and $\Delta F_{p,C,d2}$ is the difference between $F_{p,C,d2}$ and $F_{p,C,d1}$. On the basis of six tested specimens (18 bolts), it can be concluded that the losses of preload force are lower than 1.5 %.

Table 10. Losses of preload force in HV bolts caused by cyclic loading

Specimen label	Bolt label	$F_{p.C.d1}$ [kN]	$F_{p.C.d2}$ [kN]	$\Delta F_{p.C.d2}$ [%]	Mean value [%]
D3	D50C11	157.9	155.3	1.69	1.26
	D50C12	164.1	163.2	0.60	
	D50C13	165.0	162.5	1.49	
D6	D70C11	154.5	154.5	0.00	0.13
	D70C12	135.3	135.2	0.09	
	D70C13	114.8	114.5	0.29	
D9	D90C11	144.7	141.9	1.93	1.36
	D90C12	132.6	130.7	1.41	
	D90C13	190.4	189.0	0.75	

Table 11. Losses of preload force in HBT bolts caused by cyclic loading

Specimen label	Bolt label	$F_{p.C.d1}$ [kN]	$F_{p.C.d2}$ [kN]	$\Delta F_{p.C.d2}$ [%]	Mean value [%]
H3	H55C11	114.6	113.4	0.97	1.10
	H55C12	108.6	108.0	0.57	
	H55C13	127.6	125.4	1.77	
H6	H70C11	166.5	166.5	0.00	0.84
	H70C12	138.1	137.1	0.69	
	H70C13	174.1	170.9	1.84	
H9	H85C11	176.2	174.4	1.02	0.53
	H85C12	175.3	174.7	0.39	
	H85C13	171.8	171.6	0.17	

If micro settling in the bolt thread zone (in the case of HV bolts) and on the surface of steel plates during cyclic loading is taken into account, then the influence of cyclic loading on the loss of preload force is not of great significance.

An up to 5 % decrease of preload force can occur during cyclic loading of the specimens, depending on the steel plates' thickness and maximum cyclic force value. However, this decrease is momentary (only during cyclic loading) and is strictly a consequence of the lateral contraction of steel plates caused by the cyclic force acting on the specimens. During application of cyclic load, there is no yield of the steel plates' cross-section; hence, after the end of the cyclic loading, there is a relaxation of steel plates in the connection. Thus, the preload force in the bolts practically returns to its initial value.

In research made by C. Heistermann [2], the cyclic loading spectrum was defined so that the force gradually increased until specimen failure. The fatigue failure of the specimens occurred before the projected number of cycles, i.e., during cyclic loading. Based on the results obtained by measuring preload force in the bolts, the author concluded that average losses caused by cyclic loading amounted to 5.01 %. This conclusion is based on preload force values measured immediately before failure of the specimens, which raises the question of its reliability and accuracy. Namely, this conclusion ignores the fact that under the maximum axial force (defined by the cyclic load spectrum) there is lateral contraction of the specimen's steel plates, which is very significant for this phenomenon. In order to obtain a real measure of the losses of preload force, the specimens should have been unloaded after each 50 000 cycles, as that would have enabled neutralization of elastic lateral contractions of the steel plates and the measurement of the actual level of preload force in the bolts. This type of research can lead to a wrong conclusion about the effects of cyclic loading on losses of preload force, based on their values immediately before failure, since in that case it is not possible to determine which portion of the preload force loss is a consequence of lateral contraction of steel plates in the connection.

4. Conclusions

The loss of preload forces occurred in all preloaded bolts regardless of their length, size, and surface treatment of the plate assembly. There is a significant number of influences that cause bolt relaxation although, for joints in civil engineering structures, the main reasons for bolt relaxation are elastic interactions, embedment, static and cyclic loading, and long-term relaxation or creep.

The impact the cyclic loading has on the loss of preload forces in the high strength bolt (HV) and Lockbolt (HBT) was assessed using an experimental procedure based on the assumption that limiting the stress range in the specimen corresponds to 75 % of the value defined as the limit for detail class 112 [33] (realistic serviceability state scenario during a structure's lifecycle).

Based on the performed experiments involving a range of

parameters and perfect alignment between the plates, the following conclusions are given:

The application of the "Resist 86" zinc-silicate coating is a very efficient corrosion protection of friction connections. The best results, in terms of the slip factor, were obtained by installing structural elements 7–10 days after application of the coating. In this way, a slip factor of $0.45 \leq \mu \leq 0.50$ is achieved on the friction surfaces, which is sufficient to categorize these connections as roughness classes A or B according to EN 1993-1-8.

The maximum preload achieved during installation is rather consistent having the coefficient of variation of 4.6 % and 10.8 % for HBT and HV bolts, respectively.

A major part of the preload losses occurs in the first two seconds after HBT bolt installation, and in the first 10 seconds after HV bolt installation. The preload losses are up to 6,9 % and 42 % for HV and HBT bolts, respectively. These initial preload losses dominantly depend on installation methods, which are different for these two types of bolts.

Short-term losses of preload are recorded twelve hours after bolt installation. Regardless of the bolt type used, the influence of plate corrosion protection on these losses is negligible for all considered plate thicknesses.

The influence of cyclic loading, under which there is no yield or slip of connecting elements, on the preload loss in HBT and HV bolts, can be neglected. The losses of preload force are lower than 1.5 %.

Acknowledgements

This investigation is supported by the Serbian Ministry of Education, Science and Technological Development in the scope of the project 200092. The authors extend their thanks to the companies and individuals who supported this research financially and by providing the necessary material: "Alcoa Fastening Systems" (Telford, England), "Amiga" (Kraljevo, Serbia), "Armont SP" (Belgrade, Serbia), "Bata-Mat" (Belgrade, Serbia), "Euris" (Belgrade, Serbia), "INM" (Arilje, Serbia), "Johannes Steiner GmbH & Co." (Weningen, Germany), "Jotun" (Norway), "Lim inženjering" (Belgrade, Serbia), "Mašinoprojekt Kopring" (Belgrade, Serbia), "Modipack" (Požega, Serbia), "Mostogradnja" (Belgrade, Serbia), "NB Celik" (Batajnica, Serbia), "PERI oplate" (Šimanovci, Serbia) "RT Trans" (Belgrade, Serbia), and "Xella Serbia" (Vreoci, Serbia).

REFERENCES

[1] Sedlacek, G, Kammel, C.: Zum Dauerverhalten von GV-Verbindungen in verzinkten Konstruktionen – Erfahrungen mit Vorspannkraftverlusten, Stahlbau, 70 (2001) 12, pp. 917–926.

[2] Heistermann, C.: Behaviour of Pretensioned Bolts in Friction Connections. Licentiate Theses, Luleå University of Technology, 2011.

[3] Abid, M., Khalil, M.S., Wajid, H.A.: An Experimental Study on the Relaxation of Bolts. IIUM Eng J, 16 (2015) 1, pp. 43–52.

[4] Nassar, S.A., Shoberg, R.S.: Effect of Fastener Tightening Beyond Yield on the Behavior of Bolted Joints Under Service Loads, Proceeding of the 18th Annual Conference of the AMSE, Michigan State University, East Lansing, MI, pp. 1–17, 1992.

[5] Bickford, J.H.: An introduction to the design and behaviour of bolted joints -3rd edition, revised and expanded. New York: Marcel Dekker, 1995.

[6] Yang, J., DeWolf, J.T.: Mathematical Model of Relaxation in High-Strength Bolted Connections. J Struct Eng, 125 (1999), pp. 803–809.

[7] Fisher, J.W., Struik, J.H., Kulak, G.L.: Guide to design criteria for bolted and riveted joints. New York: Wiley, 1974.

[8] Yang, J.: Relaxation of high-strength bolted connections with galvanized steel, MSc thesis, University of Connecticut, Storrs, CT, 1997.

[9] DeWolf, J.T., Yang, J.: Relaxation in high-strength bolted connections with galvanized steel, Final report, Project 96-4, JHR 98-262University of Connecticut, Storrs, CT, 1998.

[10] Yang, J, DeWolf, J.T.: Relaxation in High-Strength Bolted Connections Using Galvanized Steel. J Bridge Eng 2000, 5(2):99–106.

[11] Cruz, A., Simões, R., Alves, R.: Slip factor in slip resistant joints with high strength steel. J Constr Steel Res, 70 (2012), pp. 280–288.

[12] Annan, C.D., Chiza, A.: Slip resistance of metalized–galvanized faying surfaces in steel bridge construction. J Constr Steel Res, 95 (2014), pp. 211–219.

[13] Annan, C.D., Chiza, A.: Characterization of slip resistance of high strength bolted connections with zinc-based metallized faying surfaces. Eng Struct, 56 (2013), pp. 2187–2196.

[14] Popovska, M., Petreski, B., Cvetanovski, P., Popovski, D.: Experimental procedure for slip factor determining at connections with preloaded bolts. e-GFOS 5, 8 (2014), pp. 37–43.

[15] D'Aniello, M., Cassiano, D., Landolfo, R.: Monotonic and cyclic inelastic tensile response of European preloadable gr10.9 bolt assemblies, Journal of Constructional Steel Research, 124 (2016), pp. 77–90.

[16] Cavallaro, G.F., Latour, M., Francavilla, A.B., Piluso, V., Rizzano, G.: Standardised friction damper bolt assemblies time-related relaxation and installed tension variability, Journal of Constructional Steel Research 141 (2018), pp. 145–155.

[17] D'Antimo, M., Latour, M., Cavallaro, G.F., Jaspart, J.P., Ramhormozian, S., Demonceau, J.F.: Short- and long- term loss of preloading in slotted bolted connections, Journal of Constructional Steel Research, 167 (2020), pp. 105956.

[18] Li, D., Uy, B., Wang, J., Song, Y.: Behaviour and design of high-strength Grade 12.9 bolts under combined tension and shear, Journal of Constructional Steel Research, 174 (2020), pp. 106305.

[19] Jovanović, Đ.: Behaviour of end-plate moment connections with four bolts per row, PhD thesis, University of Novi Sad, Faculty of technical sciences, 2020.

[20] Jovanović, Đ., Mitrović, N., Marković, Z., Vilotić, D., Kosić, B.: Experimental and Numerical Investigation of the T-Stub Elements with Four Bolts in a Row Until Bolt Fracture, Proceedings of the International Conference of Experimental and Numerical Investigations and New Technologies, CNNTech 2019, pp. 305-322.

[21] Stranghöner, N., Jungbluth, D., Abraham, C., Söderman, A.: Tightening behaviour of preloaded stainless steel bolting assemblies. Steel Constr, 10 (2017) 4, pp. 319–332.

[21] Stranghöner, N., Jungbluth, D., Abraham, C., Söderman, A.: Tightening behaviour of preloaded stainless steel bolting assemblies. Steel Constr, 10 (2017) 4, pp. 319–332.

[22] Fric, N.: Theoretical and experimental research of losses of pretension force in high strength bolts, doctoral thesis, University of Belgrade Faculty of civil engineering, 2015.

[23] EN1993-1-8 - Eurocode 3: Design of steel structures – Part 1-8: Design of Joints, Brussels, CEN, 2005.

[24] EN 14399-4. High strength structural bolting for preloading - Part 4: System HV -Hexagon bolt and nut assemblies, Brussels, CEN, 2015.

[25] EN ISO 898-1. Mechanical properties of fasteners made of carbon steel and alloy steel — Part 1: Bolts, screws and studs with specified property classes — Coarse thread and fine pitch thread. Brussels, CEN, 2009.

[26] EN ISO 6892-1. Metallic materials – Tensile testing. Part 1: Method of test at room temperature. Brussels, CEN, 2009.

[27] EN 1090-2. Execution of steel structures and aluminium structures – Part 2: Technical requirements for steel structures, Brussels, CEN, 2008.

[28] EN ISO 16047. Fasteners - Torque/clamp force testing. Brussels, CEN, 2005.

[29] ISO 8501-1. Preparation of steel substrates before application of paints and related products — Visual assessment of surface cleanliness — Part 1: Rust grades and preparation grades of uncoated steel substrates and of steel substrates after overall removal of previous coatings, International organization for standardization, Brussels, CEN, 2007.

[30] EN 14399-4:2005: High-strength structural bolting assemblies for preloading - Part 4: System HV - Hexagon bolt and nut assemblies, Brussels, CEN, 2015.

[31] Husson, W.: Friction Connections with Slotted Holes for Wind Towers. Licentiate Theses, Luleå University of Technology, 2008.

[32] Schließringbolzensysteme - Berechnung von Verbindungen nach Eurocode 3 und VDI 2230, DVS-Deutscher Verband für Schweißen und verwandte Verfahren e. V. und EFB-Europäische Forschungsgesellschaft für Blechverarbeitung e. V., 2016.

[33] EN 1993-1-9: 2005, Eurocode 3: Design of steel structures – Part 1-9: Fatigue, Brussels, CEN, 2005.